

APPLICATION OF VERIFICATION METHODS ON A COMPLEX FLOW FIELD CALCULATED BY LARGE-EDDY SIMULATION: BLOOD PUMP FLOW

LUCAS KONNIGK^{1*}, BENJAMIN TORNER^{1*} AND FRANK-HENDRIK WURM¹

¹Institute of Turbomachinery
University of Rostock
Albert-Einstein-Str. 2, 18059 Rostock, Germany
lucas.konnigk@uni-rostock.de
www.itu.uni-rostock.de

Key words: Verification, Large-Eddy Simulation, Blood Pumps.

Abstract. Ventricular Assist Devices (VADs) are the most promising treatment option of end-stage heart failure. These usually continuous-flow pumps are used to bridge the gap between needed and available donor hearts. Unfortunately, most patients with implanted VADs are suffering from adverse events due to flow induced blood damage. These events can be attributed to blood components (red blood cells, platelets, proteins) in contact with crucial shear fields in the pump. Regarding this, it is common to predict blood damage via computational fluid dynamics (CFD) nowadays. Therefore, we calculated the flow within an axial VAD prototype with ANSYS CFX and the Large Eddy Simulation (LES) method on a 100M element mesh with the aim to achieve a more sufficient calculation of transient velocity gradients, i.e. shear stresses, as with high-dissipative turbulence models. The CFD solution needs to be verified, but grid convergence studies of arbitrary flow quantities for solution verification are not useful for LES, due to the direct correlation between turbulence model activity and grid spacing, i.e. filter width. Therefore, we used four alternative verification methods. The first examines the influence of the numerical diffusion and based on these results, an LES index of quality is derived. Secondly, we compare the internal flow losses due to dissipation and turbulence production against hydraulic losses, determined from the pump characteristics to examine, whether the LES is able to capture the turbulent flow losses. Third, we compared resolved vs. modelled turbulent kinetic energy (TKE) and finally, we analyzed TKE spectra in the flow field. Our objective is to present the application of different methods for LES verification of complex flow fields, in which a sufficiently fine temporal and spatial resolution of highly mesh-sensitive quantities is very important. We compared methods in means of consistency among each other and especially regarding the presumable correctness of the numerical blood damage prediction.

1 INTRODUCTION

Heart insufficiency and especially heart failure are one of the most common diseases and over five million people are affected by this in the USA alone [1]. Approximately 4,000

* The authors Lucas Konnigk and Benjamin Torner contributed equally to this work

thousand of those patients have end-stage heart failure, which means that they need an urgent heart transplant, but only 3,000 donor organs are available worldwide per year [2,3]. This gap between needed and available heart transplants resulted in technical solutions. The most promising treatment option for end-stage heart failure are Left Ventricular Assist Devices (LVADs) with approximately 12,000 implants between 2006 and 2014 captured by the Interagency Registry for Mechanically Assisted Circulatory Support (INTERMACS) [4]. Figure 1 shows an exemplary pump with the typical intracorporeal arrangement for LVADs.

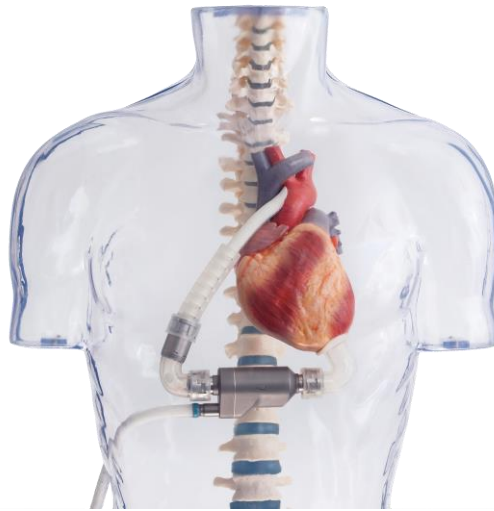


Figure 1: Axial continuous-flow LVAD INCOR® from Berlin Heart GmbH

The blood flows from the left ventricle in the pump which generates the pressure for the body's circulation system and exits through an outflow cannula into the aorta (from right to left in Figure 1). With the current continuous-flow devices, rates of survival for one and two year support are 80% and 70%, respectively [4]. Heart pumps are designed to bridge the time until a heart transplant is available ("bridge to transplant") or even for long time support ("destination therapy"). Even though LVADs are a promising option for the treatment of heart failure, only 30 percent of patients were free from complications and major adverse events like infection, bleeding, device malfunction, stroke or death within the first twelve months [4]. Bleeding and strokes in addition with hemolysis (damage of red blood cells) can be related to flow-induced blood damage due to the non-physiological flow environment within the pump [5]. Shear stresses and the associated exposure times can cause damage to the blood particles, which might lead to the described events [6].

Regarding that, the flow prediction in pumps with Computational Fluid Dynamics (CFD) is a common-used technique to identify and minimize the blood damage potential by evaluating the acting shear stresses in a specific device [7–13]. Today, numerical blood damage prediction is confined under usage of Unsteady Reynolds-Averaged Navier-Stokes simulations (URANS) in addition with eddy viscosity-based two-equation models, because of the relatively low computational effort. When performing grid convergence studies with such URANS simulation, it can be seen that calculated velocity gradients, i.e. shear stresses, need further grid

refinement, whereas integral quantities like pressure heads are in the asymptotic range of grid convergence. With Large Eddy Simulation (LES) methods and less dissipative turbulence models, discretization schemes and finer grids, a quantitatively more correct calculation of shear stresses and hence blood damage prediction could be possible. Unfortunately, a solution verification obtained with LES is more difficult as with URANS. One reason is the direct dependence of turbulence model activity and grid size, so that it is difficult to segregate discretization and modelling errors from each other [14].

Aim of this study is to applicate common literature methods for LES solution verification on a complex flow field ranging from laminar, transitional to turbulent flow. Additionally, we want to show a procedure, with which it is possible to indicate, whether turbulent flow losses are accurately resolved and modeled. Because of the dependence between dissipation and velocity gradients, this also indicates, whether shear stresses are calculated globally correct.

2 MATERIAL AND METHODS

2.1 Geometry and computational setup

The considered heart pump is an axial flow pump designed by our institute with a five-bladed inlet guide vane, two rotor blades and with three blades in the outlet guide vane. The geometry is shown in Figure 1a and it was designed with the objective to analyze turbulent flow phenomena in heart assist devices. The actual inlet of the flow domain was defined four rotor diameters and the outlet seven diameters away from the pump to prevent that boundary conditions negatively influence the flow within the pump. A zero total pressure condition was defined at the inlet and a flow rate of $Q = 4.5 \text{ l min}^{-1}$ was specified at the outlet. The rotor speed was 7,900 rpm and time-averaging was done for 10 revolutions after RMS residuals were lower than 10^{-5} and all monitored values, e.g. pressure head, were statistically converged. The fluid density was $\rho = 1050 \text{ kg/m}^3$ with a dynamic viscosity of $\mu = 0.0035 \text{ Pa} \cdot \text{s}$. The assumption of a Newtonian fluid is valid for most VADs, because the viscosity is almost constant above shear rates of 100 s^{-1} [15]. The smallest turbulent scales were modeled with the dynamic Smagorinsky model with a bounded Smagorinsky parameter between $C_{DS} = 0 \dots 0.3$. Because of the adaption of the Smagorinsky constant to the flow, the model is automatically valid for laminar regimes, e.g. in the inlet cannula, and no near-wall corrections are needed [16]. The rotor's rotation was simulated with multiple reference frames and transient sliding interfaces between guide vanes and rotor. Previous simulations were performed to determine turbulent inflow boundary conditions. Turbulent intensity and eddy length scale were estimated from empirical correlations for turbulent pipe flow ([17]). These results were compared to solutions, where none or high turbulence was specified at the inlet. The results showed no significant difference between mean field and integral quantities and let us conclude to neglect any time-dependent fluctuations at the inlet for the LES.

2.2 Discretization

The hexahedral and block-structured mesh was created with ICEM CFD 18.0 (ANSYS, Inc., Canonsburg, USA) and examples of the mesh can be seen in Figure 1b. It was build using literature recommendations ([16,18]) for wall-resolving LES. Regarding that, the grid space in flow direction Δx , spanwise direction Δz and in wall normal direction Δy were adjusted until the

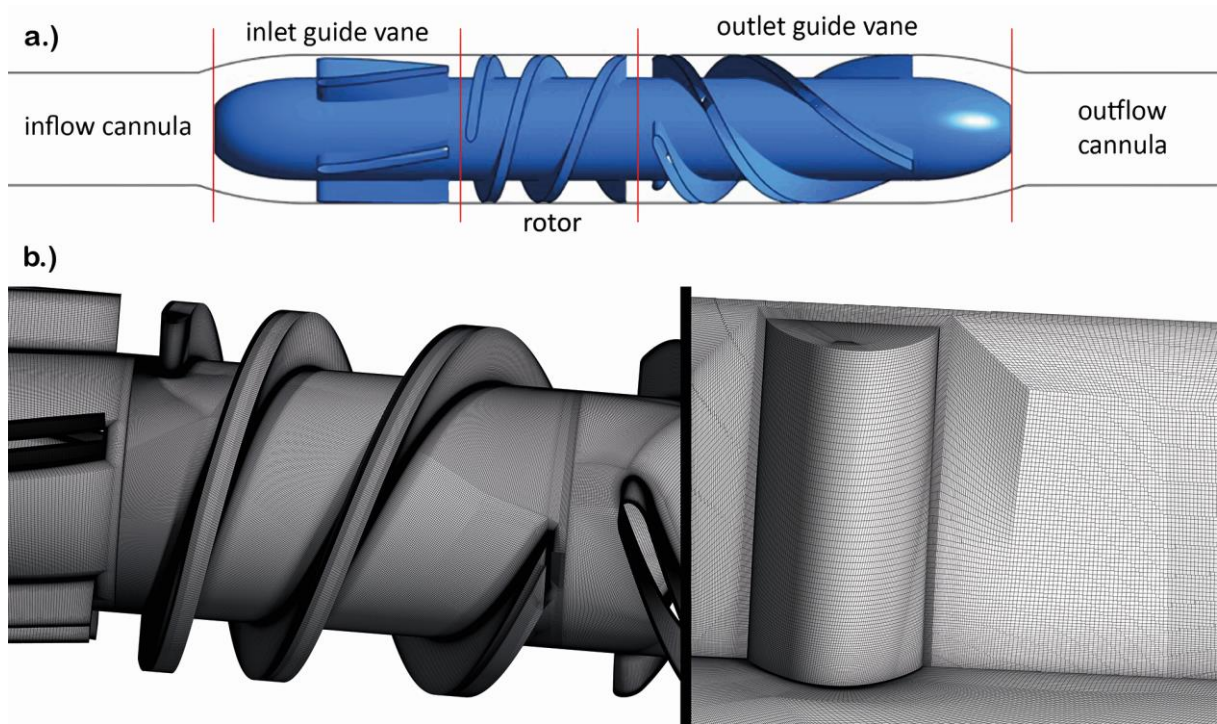


Figure 2: a.) Computational domain b.) Surface mesh of the rotor plus parts of inlet and outlet guide vane on the left and volume mesh of a selected plane near rotor leading edge

near-wall mesh fitted the upper limits of the dimensionless wall coordinates $x^+ = (\Delta x \cdot (\tau_w/\rho)^{0.5}/\nu = 50$, $z^+ = 15$ and $y^+ = 1$, calculated with wall shear stress τ_w and kinematic viscosity ν . The mesh growth factor away from the wall is $r_g = 1.05$. Higher values of $y^+ \approx 1.4$ were only tolerated at small locations at the guide vanes to prevent much higher mesh sizes. Grid angles of the resulting mesh are greater than 23° with aspect ratios smaller than 41. Aspect ratios are in a range between one and five in the core region of the flow. The clearance between rotor and casing is $120 \mu\text{m}$ and was discretized with 28 and 74 elements in height and width, respectively. The final mesh for the LES calculations has a size of 105 million elements.

ANSYS CFX 17.1 was used to solve the three-dimensional Navier-Stokes equations by the finite volume method. The governing equations were spatially discretized by a second order central differencing scheme (CDS). The CDS was bounded to prevent numerical oscillations due to high gradients, i.e. “wiggles”. The transient term was discretized by a second order backward scheme and the timestep equals a rotational increment of 0.36° , which are approximately $53 \mu\text{s}$. This resulted in a RMS Courant number of 0.4.

2.3 Solution verification

Grid convergence studies and uncertainty estimations (as in [19]) are developed for RANS methods and cannot be easily applied to LES computation, since the modeling and discretization error are directly related with LES. Hence, other methods are needed to evaluate the correct calculation of governing equations. Because of the complexity of the flow field, our aim was to choose verification methods from the literature, which are applicable with relatively low effort to obtain sufficient statements regarding the solution verification. Therefore, we

chose pointwise, single-grid and multigrid verification strategies. Sometimes, solutions on multiple grids cannot be done with LES, because of the immense computing time for computations of engineering interest [14]. For this reason, single-grid estimators are an important tool for solution verification. The pointwise method we chose is the analysis of turbulent kinetic energy (TKE) spectra in turbulent flow regimes, e.g. gap vortex region. Aim of LES is to resolve the turbulent flow field up to the inertial subrange of the energy cascade [18]. This range is indicated by a slope of $f^{-5/3}$ in the spectrum. The resolution up to the inertial subrange is one condition for the use of algebraic turbulence models like the Smagorinsky model. As opposed to very complex two-equation models, only small scale fluctuations need to be modeled in the unresolved subgrid scale (SGS) stress [18]. Those scales are less energy containing and meant to be isotropic [20]. Therefore, the use of less complex turbulence models should be justified, if the condition is fulfilled.

To identify possible regions with a lack of resolution, field-dependent verification methods are needed. One simple approach is to compare resolved TKE k_{res} to the total TKE k_{tot} . The modeled TKE is estimated by following equation [21]:

$$k_{SGS} \approx \left(\frac{\nu_t}{C_{DS}\Delta} \right)^2, \quad (1)$$

with eddy viscosity ν_t and filter width $\Delta = \sqrt[3]{\Delta x \Delta y \Delta z}$. The resulting ratio between resolved to total TKE can now be written as:

$$\frac{k_{res}}{k_{tot}} = \frac{k_{res}}{k_{res} + k_{SGS}}. \quad (2)$$

If solutions on multiple grids are available, Celik et al. [22] reported several indices of quality for LES. One index compares the fluid viscosity ν to the effective viscosity $\nu_{eff} = \nu + \nu_t + \nu_{num}$, which results from the damping of velocity gradients due to the numerical approximation of the gradients. This approximation in combination with the eddy viscosity leads to the effective viscosity of the calculated flow field, since the real velocity gradients are not fully resolved. The numerical viscosity can be obtained by:

$$\nu_{num} \approx C_\nu \Delta \sqrt{k_{num}} \quad (3)$$

with the assumption that ν_t is proportional to ν_{SGS} . The constant C_ν is set to be 0.165 [23]. With the numerical TKE, the total TKE expands to $k_{tot} = k_{res} + k_{SGS} + k_{num}$. The modeled and numerical TKE can be summarized to the effective SGS turbulent kinetic energy $k_{eff_SGS} = k_{SGS} + k_{num}$. This value can be estimated in means of a Richardson extrapolation [22]:

$$k_{eff_SGS}^1 = a_k h_1^p \quad (4)$$

$$k_{eff_SGS}^2 = a_k h_2^p \quad (5)$$

The indices 1, 2 are representing the solution on the fine (1) and coarse (2) grid, respectively. The local grid size h equals to the filter width from Eq. (1) and p is the order of grid convergence and is assumed to be 2, because of the second order spatial and temporal discretization schemes. The constant a_k is than calculated from:

$$a_k = \frac{1}{h_1^p} \left[\frac{k_{res}^1 - k_{res}^2}{\alpha^p - 1} \right] \quad (6)$$

where $\alpha = h_2/h_1 > 1$ is the grid refinement parameter. The numerical TKE in Eq. (3) can now be calculated by $k_{num} = k_{eff_SGS} - k_{SGS}$. Finally, the LES index of quality based on the effective viscosity LES_IQ_v can be calculated by:

$$LES_IQ_v = \frac{1}{1 + \alpha_v \left(\frac{\langle v_{eff} \rangle}{\nu} \right)^n} \quad (7)$$

Following [22], the parameters are $\alpha_v = 0.05$ and $n = 0.53$ to ensure that LES_IQ_v ranges between 0 ... 1.

A second coarser grid is necessary for this verification method. Therefore, we scaled down the fine grid in every spatial direction to guarantee geometrical similarity. This coarse mesh has approximately 33 million grid nodes and the simulation was performed by the same computational setup as for the fine grid.

2.3.1 Power Loss Analysis (PLA)

The Power Loss Analysis (PLA) is used to verify the LES in a global way. This method gives information, whether the mesh resolution and CFD setup is capable of resolving the internal losses within the domain adequately. As a common-used technique, the turbulent flow field is treated in a statistical framework and is separated into the mean quantities $\langle \phi \rangle$ and fluctuations ϕ' . In the PLA, the total loss of the time-averaged flow field is compared using two equations. The first one, Eq. (13), is the total power loss $P_{Loss,1}$ calculated by the deviation between the drive power of the blades P_{blades} and the increase of the hydraulic power ΔP_{Fluid} . These terms include the blades moment M_{blades} , angular velocity ω , total pressure increase Δp_{tot} and the flow rate Q :

$$P_{Loss,1} = P_{blades} - \Delta P_{Fluid} = M_{blades} \cdot \omega - \Delta p_{tot} \cdot Q \quad (8)$$

The total power loss P_{Loss} can also be determined by integrating all internal losses within the pump which contribute to P_{Loss} . The flow energy of the mean motion is reduced by two loss shares [24]. The first one is the loss because of direct dissipation ε_{dir} :

$$P_{dir} = \rho \int_V \varepsilon_{dir} dV = \rho \int_V \nu \left\langle \frac{\partial u_i}{\partial x_j} \right\rangle \left(\left\langle \frac{\partial u_i}{\partial x_j} \right\rangle + \left\langle \frac{\partial u_j}{\partial x_i} \right\rangle \right) dV \quad (9)$$

The direct dissipation describes the transfer from kinetic energy of the mean field into heat. The second energy loss for the mean flow is the production of turbulent kinetic energy k_{prod} [20]. Integrated over the whole domain, the resolved turbulent losses are:

$$P_{turb,res} = \rho \int_V -\langle u'_i u'_j \rangle \left\langle \frac{\partial u_i}{\partial x_j} \right\rangle dV = \rho \int_V k_{prod} dV \quad (10)$$

Since LES is not resolving the whole spectrum of velocity fluctuations, a modeled quantity is necessary to complement the energy loss for the mean motion. To include the TKE production from the small unresolved scales and regarding the equilibrium between production and dissipation, it is possible to include the modeled turbulent dissipation $\varepsilon_{turb,mod}$ in order to complete the loss for all turbulent scales:

$$P_{turb,mod} = \rho \int_V \varepsilon_{turb,mod} dV = \rho \int_V \nu_t \left\langle \frac{\partial u_i}{\partial x_j} \left(\frac{\partial u_i}{\partial x_j} + \frac{\partial u_j}{\partial x_i} \right) \right\rangle dV \quad (11)$$

Finally, the total power loss due to the internal losses of the flow $P_{Loss,2}$ can be written as:

$$P_{Loss,2} = P_{dir} + P_{turb,res} + P_{turb,mod} \quad (12)$$

In theory, Eq. (8) and (12) should lead to the same result. If this condition is fulfilled, it can be concluded the computational setup in combination with the discretization is appropriate to resolve the internal flow losses by the terms P_{dir} , $P_{turb,res}$ and $P_{turb,mod}$. The deviations between Eq. (8) and (12) for the Large Eddy Simulations within the pump will be compared.

3 RESULTS

3.1 Resolution of turbulent kinetic energy (TKE)

Figure 3 shows two velocity fluctuation spectra at different points in the pump. One time series was taken in the gap vortex region in the rotor (left) and the other in the channel of the outlet guide vane (right). It can be seen, that the turbulent scales in the outlet guide vane contain

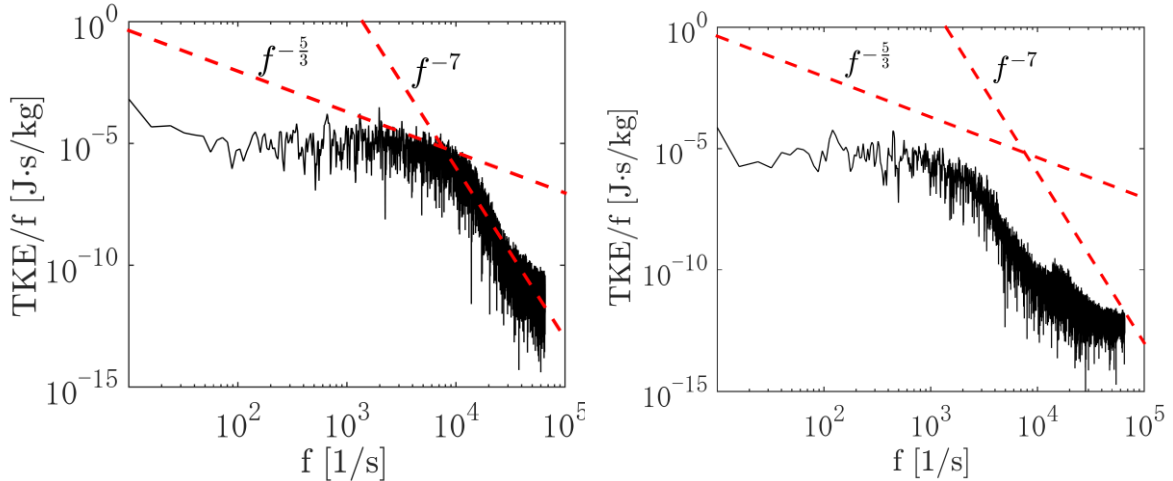


Figure 3: TKE spectra at two locations within the pump. On the left: time-series taken from the gap vortex region in the rotor. On the right: point in the channel of the outlet guide vane. The red dotted lines indicate the characteristic slopes $f^{-\frac{5}{3}}$ and f^{-7} of the inertial subrange and dissipation range, respectively.

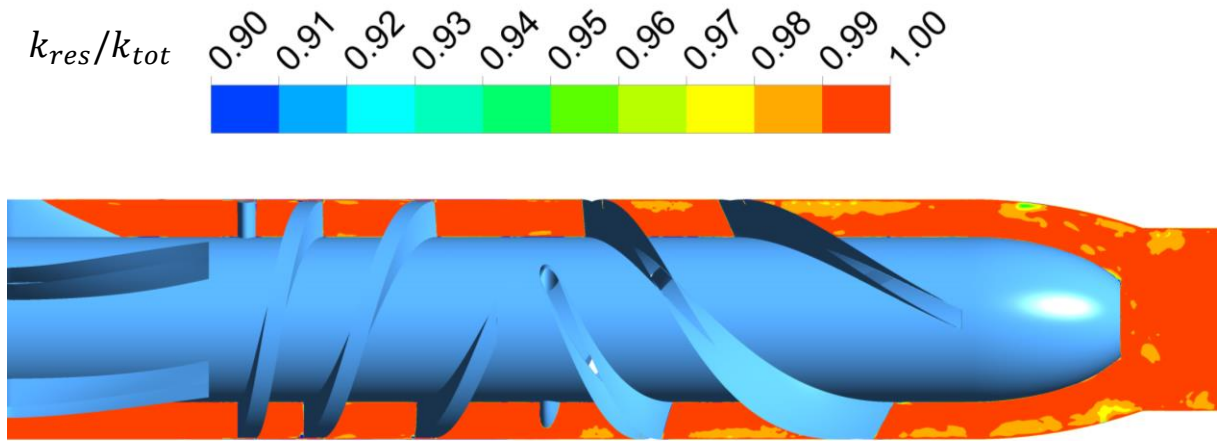


Figure 4: Time-averaged resolved versus total TKE in a cut-plane through the pump.

less energy as in the rotor and that the energy is dissipating earlier. It can be seen for both time series, that the inertial range of the energy cascade, indicated by a slope of $f^{-5/3}$, is resolved properly. Even the slope of f^{-7} can be identified in the spectra. In this range, i.e. at higher frequencies, small vortices transfer their energy into heat by turbulent dissipation [25]. Figure 4 shows the ratio of the time-averaged resolved and computed total turbulent kinetic energy calculated with Eq. (2) in a cut plane within the pump. It can be seen, that $k_{res}/k_{tot} > 0.9$ in the entire plane observed in Figure 4. Much smaller ratios can only be found in the inflow cannula, because of the laminar flow in this region. However, aim of an LES is to resolve the turbulent flow field to (80 ... 90)% and this seems to be accomplished in the crucial areas indicated by this method [20,26].

A more reliable verification method is the use of multiple solutions on different meshes. Using the open source software ParaView 5.2.0 (Kitware, Inc., New York, USA), we resampled the time-averaged solution of our coarse grid on the nodes of the fine grid and calculated the LES_{IQ_v} using Eq. (3-7). Figure 5 shows this index in a cut plane through the pump. The LES_{IQ_v} is greater than 0.9 in the whole pump. In contrast to the single-grid ratio in Fig. 4, Figure 5 displays irregularities in the resolution of TKE. The LES_{IQ_v} shows higher and homogeneous distributed values in the inflow cannula. A global minimum of the index can be found in the wake of the hub. In general, the LES_{IQ_v} decreases with increasing turbulence, which is first massively introduced by the motion of the rotor. Another difference between both methods is

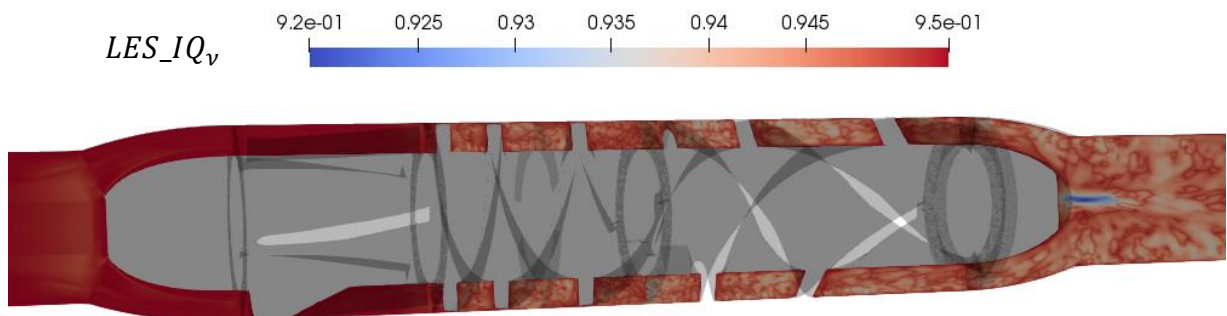


Figure 5: LES index of quality LES_{IQ_v} calculated with modeled and numerical TKE in a cut plane through the pump in a range of 0.92 ... 0.95.

that the LES_{IQ_v} includes the influence of numerical diffusion.

Another approach to visualize the influence of modeling and numerical, i.e. discretization, error is to compare different Reynolds numbers Re , which are calculated with the different viscosities, similar to the LES_{IQ_v} approach (Eq. (13))

$$Re_{eff} = \frac{\langle U \rangle \cdot h}{\nu + \langle \nu_t \rangle + \langle \nu_{num} \rangle} \quad Re_{num} = \frac{\langle U \rangle \cdot h}{\nu + \langle \nu_{num} \rangle} \quad Re_{SGS} = \frac{\langle U \rangle \cdot h}{\nu + \langle \nu_t \rangle} \quad (13)$$

The effective Reynolds number Re_{eff} represents the “true” computed Re of the calculated flow in opposite to the “real”/exact flow problem, because of velocity gradient damping due to SGS stress (ν_t) and numerical approximations of the partial differential equations on a three-dimensional grid (ν_{num}). Figure 6 shows the comparison of different ratios between the Reynolds numbers from Eq. (13) and Re only calculated with the fluid viscosity in the wake of the hub. This part was chosen of the domain was chosen, because previous analysis indicated a local maximum of numerical errors at this location. Figure 6 shows that the overall ratio between normal Re and Re_{eff} is in a range between 1 and 2.3. Furthermore, the different behavior between modeling and discretization error can be seen. Whereas the numerical viscosity reflects the local error maximum in the wake, the eddy viscosity displays other locations of maximum values. It seems, that the flow in this region is mostly influenced by the discretization error, since the ratio of Re/Re_{SGS} is not exceeding 1.2.

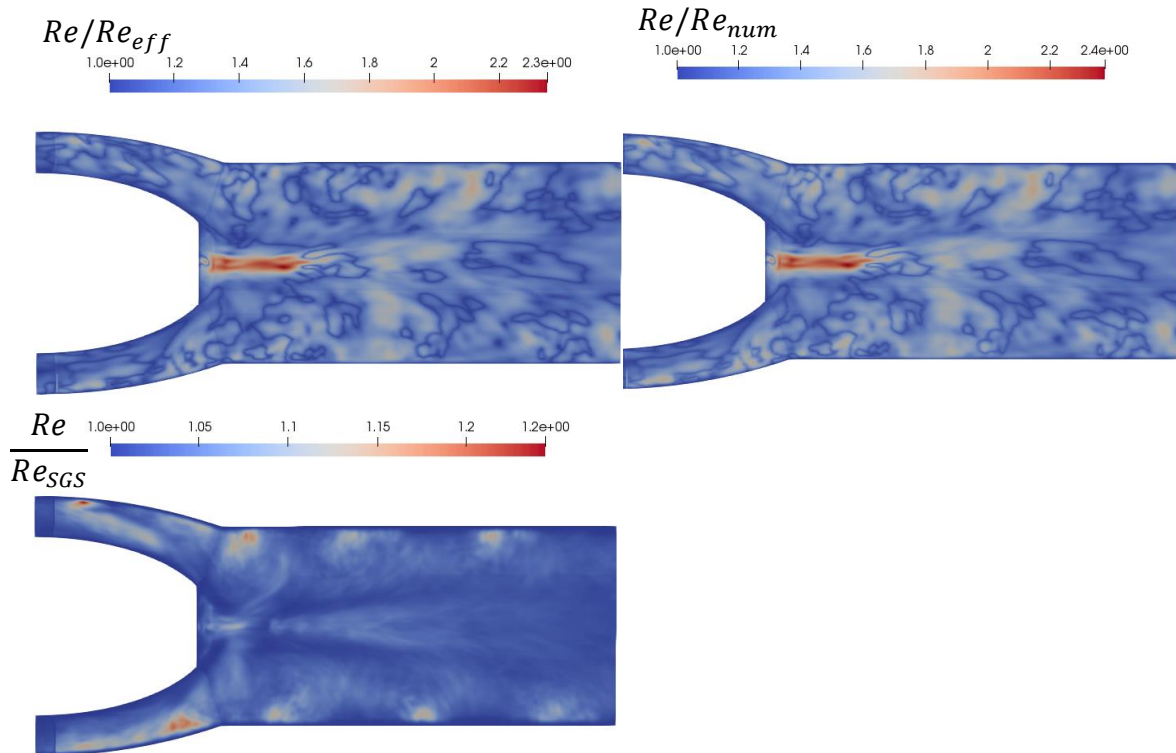


Figure 6: Comparison of ratios between different Reynolds numbers calculated with Eq. (13) in the wake of the hub.

3.2 PLA results

The power loss calculated by the drive power and increase of hydraulic power (Eq. (8)) is $P_{Loss,1} = 1.493 \text{ W}$. The loss calculated by integrating all internal flow losses within the pump over the pump volume (Eq. (9-12)) is $P_{Loss,2} = 1.469 \text{ W}$. The deviation between the two values is $(P_{Loss,1} - P_{Loss,2})/P_{Loss,1} = 0.016$ or 1.608%. By analyzing the different loss shares of Eq. (12), it can be seen that the gross of the power loss comes from direct dissipation with a share of 78.83% (1.158 W). The loss due to turbulence production amounts 19.45% (0.286 W) and the influence of subgrid scale stress on the total power loss is 1.721% (0.025 W). The comparison of the resolved and modeled turbulent losses reveals, that approximately 92% of turbulence is directly resolved by this LES.

4 DISCUSSION

Aim of this paper was to apply relatively easy-to-use verification methods for an LES computation to analyze, if a reliable solution verification is possible, when no experimental or direct numerical simulation (DNS) data are available and without increasing the computational effort by calculating additional error transport equations, since the flow regime and geometry is already very complex with a computing time of 48 hours per rotor revolution performed on a HPC cluster.

The turbulence spectra from transient three-dimensional velocity data at two different turbulent flow locations indicate that the use of an LES turbulence model is reasonable with the numerical setup. The inertial subrange of the energy cascade is adequately resolved and even the dissipation range is identifiable for both locations. This led us conclude, that the spectra are consistent with the theory of turbulence and the spatial and temporal discretization of the simulation is appropriate.

The comparison of total computed TKE to resolved TKE showed a sufficient resolution of turbulent kinetic energy by the LES with a maximum of 10 percent of modeled TKE only at small spots within the pump. However, besides the fact that sometimes single-grid methods are the only option to verify the solution, the underlying assumptions are not necessarily correct. The used prediction assumes that the calculated total TKE will not increase with further grid refinement. Nonetheless, it is an easy way to quickly evaluate the capability of the conducted LES to resolve TKE within the flow. Furthermore, the ratio can give qualitative information about a possibly needed grid refinement at locations of poor TKE resolution. The used ratio do not involves the influence of numerical diffusion due to the discretization. This was further analyzed by the LES_{IQ_v} .

The LES index of quality LES_{IQ_v} showed similar sufficient results with values always greater than 0.92. But this method has also some simplifications. Celik *et al.* [22] proposed this index with the assumption that the behavior of the effectively modeled and numerical TKE depends only on the grid size, order of convergence and a calculated constant. An implicit filtering was used in our computation, hence the grid size equals the filter size, so that the assumption is reasonable in our case. We assumed further that the order of convergence is equal to two, because of the second order discretization schemes. This is not true in all cases, since the CDS is bounded, which means that it is blending between second and first order at locations of high gradients to prevent numerical oscillations. Hence, future will be the calculation of the order of convergence p using a third solution on a coarser grid. Further discussion on this topic

can be found in [14]. The direct comparison between the Reynolds numbers which result from eddy and numerical viscosity showed, that the numerical diffusion has a greater impact on the computed flow field than the modeling error. This could be shown in a region, where the LES_{IQ_v} reveals a maximum error. The “true” Re of the flow was 2.4 times higher against the Re only calculated with the fluid viscosity itself. The numerical viscosity contributes the greatest share to this increase. Nonetheless, the influence of the numerical diffusion is relatively low compared to values from the literature [22,27].

Our last verification method was the Power Loss Analysis. The PLA compares the power losses due to drive power and the increase of hydraulic power with the internal flow losses due to dissipation and turbulence production, whereby both calculations should lead to the same value. With our LES, the difference between both terms was 1.7%. This verification can be expanded to a validation, when pressure increase and rotor’s torque are measured via the pump. With a validated power loss with the first term (Eq. (8)) and a small difference to Eq. (12), a sufficiently global computation of internal flow losses is guaranteed by the simulation. This will also be done in the nearest future

5 CONCLUSION

In this study, various methods for solution verification were applied on a Large-Eddy Simulation of a blood pumps flow. The methods intend to analyze, directly or indirectly, the resolution of turbulent kinetic energy by the numerical setup in different ways. All obtained verification results indicate, that approximately at least 90 percent of turbulent length scales are directly resolved by the performed LES. The PLA showed, that the internal turbulent flow losses are adequately resolved from a global point of view to reflect the losses determined from integral quantities like the pumps pressure head.

The field-dependent ratio between total and resolved TKE indicated only a few regions of relatively poor resolution ($k_{tot}/k_{res} \approx 0.9$) in the pump. The influence of the numerical diffusion was additionally assessed by the LES_{IQ_v} and it could be shown that the influence of the discretization prevails the activity of the turbulence model in regions of highest errors, which were indicated by the computed Reynolds numbers. At this location, the effective viscosity, as a sum of numerical, eddy and fluid viscosity, is approximately two times higher than the fluid viscosity itself. Our results show, that the numerical viscosity should not be neglected when performing an error estimation. Spectra of turbulent kinetic energy in the gap vortex region and in the channel of the outlet guide vane indicated a sufficiently fine temporal and spatial resolution to applicate the LES method, since the inertial subrange were resolved in the spectra at both points. Even the dissipation range was displayed.

Every applied method can be questionable for solution verification if utilized separately and by itself. But the results from all methods can be assessed easily without much computational effort and if all results combined together are displaying a sufficient outcome, we conclude a positive verification of the solution. This is important for simulation setups and flow environments with high computing time and geometries under engineering interest, where reliable results are needed in a short period. The source code in most commercial solvers is not accessible. In such cases and when no validation data are available, the application of the mentioned verification methods is recommended.

ACKNOWLEDGEMENTS

We acknowledge the HLRN for providing HPC resources. We want to thank Guenther Steffen, who has made a contribution to the meshing.

REFERENCES

- [1] Mancini, D. and Colombo, P.C. Left Ventricular Assist Devices: A Rapidly Evolving Alternative to Transplant. *J Am Coll Cardiol* (2015) **65**(23): 2542-2555. doi:10.1016/j.jacc.2015.04.039.
- [2] Rose Eric A. et al. Long-Term Use of a Left Ventricular Assist Device for End-Stage Heart Failure. *The New England Journal of Medicine* (2001). <http://www.nejm.org/doi/pdf/10.1056/NEJMoa012175>. Accessed January 27, 2017.
- [3] Torner, B., Hallier, S., Witte, M. and Wurm, F.-H. Large-Eddy and Unsteady Reynolds-Averaged Navier-Stokes Simulations of an Axial Flow Pump for Cardiac Support. In: ASME, ed. Proceedings of the ASME Turbo Expo 2017: Turbine Technical Conference and Exposition-2017. New York, N.Y.: ASME, 2017.
- [4] Kirklin, J.K., Naftel, D.C. and Pagani, F.D., et al. Seventh INTERMACS annual report: 15,000 patients and counting. *J. Heart Lung Transplant.* (2015) **34**(12): 1495-1504. doi:10.1016/j.healun.2015.10.003.
- [5] Graefe, R., Henseler, A. and Steinseifer, U. Multivariate Assessment of the Effect of Pump Design and Pump Gap Design Parameters on Blood Trauma. *Artificial Organs* (2016) **40**(6): 568-576. doi:10.1111/aor.12603.
- [6] Buja LM, Butany J, eds. *Cardiovascular pathology*. Fourth edition. London: Elsevier 2016.
- [7] Taskin, M.E., Fraser, K.H., Zhang, T., Gellman, B., Fleischli, A. and et al. Computational Characterization of Flow and Hemolytic Performance of the UltraMag Blood Pump for Circulatory Support. *Artificial Organs* (2010) **34**(12): 1099-1113.
- [8] Taskin, M.E., Fraser, K.H., Zhang, T., Wu, C., Griffith, B.P. and Wu, Z.J. Evaluation of Eulerian and Lagrangian models for hemolysis estimation. *ASAIO J.* (2012) **58**(4): 363-372. doi:10.1097/MAT.0b013e318254833b.
- [9] Farinas, M.-I., Garon, A. and Lacasse, D. Asymptotically Consistent Numerical Approximation of Hemolysis. *Journal of biomechanical engineering* (2006) **128**(5).
- [10] Goubergrits, L. and Affeld, K. Numerical estimation of blood damage in artificial organs. *Artificial Organs* (2004) **28**(5): 499-507. doi:10.1111/j.1525-1594.2004.07265.x.
- [11] Grigioni, M., Daniele, C., Morbiducci, U., D'Avenio, G., Di Benedetto, G. and Barbaro, V. The power-law mathematical model for blood damage prediction: analytical developments and physical inconsistencies. *Artificial Organs* (2004) **28**(5): 467-475. doi:10.1111/j.1525-1594.2004.00015.x.
- [12] Myagmar, O. and Day, S. The Evaluation of Blood Damage in a Left Ventricular Assist Device. *J. Med. Devices* (2015) **9**(2): 1-2. doi:10.1115/1.4030122.
- [13] Fraser, K.H., Zhang, T., Taskin, M.E., Griffith, B.P. and Wu, Z.J. A quantitative comparison of mechanical blood damage parameters in rotary ventricular assist devices: shear stress, exposure time and hemolysis index. *Journal of biomechanical engineering* (2012) **134**(8): 81002. doi:10.1115/1.4007092.

- [14] CELIK, I., Klein, M., FREITAG, M. and Janicka, J. Assessment measures for URANS/DES/LES: An overview with applications. *Journal of Turbulence* (2006) **7**: N48. doi:10.1080/14685240600794379.
- [15] Merrill, E.W. Rheology of blood. *Physiol Rev* (1969) **49**(4): 863-888.
- [16] Breuer, M. *Direkte numerische Simulation und Large-Eddy Simulation turbulenter Strömungen auf Hochleistungsrechnern*. [Univ., Habil.-Schr.--Erlangen-Nürnberg, 2001]. Aachen: Shaker Verlag 2002.
- [17] ANSYS Inc. *ANSYS FLUENT 12.0 User's Guide. Chap. 7.3* 2009.
- [18] Fröhlich, J. *Large Eddy Simulation turbulenter Strömungen*. 1st ed. Wiesbaden: Teubner 2006.
- [19] Eça, L.R.C. and Hoekstra, M. A procedure for the estimation of the numerical uncertainty of CFD calculations based on grid refinement studies. *Journal of Computational Physics* (2014) **262**: 104-130. doi:10.1016/j.jcp.2014.01.006.
- [20] Pope, S.B. *Turbulent flows*. Cambridge, New York: Cambridge University Press 2000.
- [21] Gerasimov A. *Quick Guide to Setting Up LES-type Simulations: Version 1.4*. [ANSYS Customer Portal: Solution 2039348]; 2016.
- [22] Celik, I.B., Cehreli, Z.N. and Yavuz, I. Index of Resolution Quality for Large Eddy Simulations. *J. Fluids Eng.* (2005) **127**(5): 949. doi:10.1115/1.1990201.
- [23] Celik, I.B., Klein, M. and Janicka, J. Assessment Measures for Engineering LES Applications. *Journal of Fluids Engineering* (2009).
- [24] Gersten, K. and Herwig, H. *Strömungsmechanik: Grundlagen der Impuls-, Wärme- und Stoffübertragung aus asymptotischer Sicht ; mit 58 Tabellen*. Braunschweig [u.a.]: Vieweg 1992.
- [25] Heisenberg, W. Zur statistischen Theorie der Turbulenz. *Z. Physik* (1948) **124**(7-12): 628-657. doi:10.1007/BF01668899.
- [26] Scillitoe, A.D., Tucker, P.G. and Adami, P. Evaluation of RANS and ZDES Methods for the Prediction of Three-Dimensional Separation in Axial Flow Compressors. In: ASME, ed. *Proceedings of the ASME Turbo Expo 2015: Turbine Technical Conference and Exposition-2015*. New York, N.Y.: ASME ,2015.
- [27] Celik, I.B. Procedure for Estimation and Reporting of Discretization Error in CFD Applications. Accessed August 30, 2016.